nature immunology

Type II natural killer T cells use features of both innate-like and conventional T cells to recognize sulfatide self antigens

Enrico Girardi[1], Igor Maricic[2], Jing Wang[1], Thien-Thi Mac[1], Pooja Iyer[1], Vipin Kumar[2] & Dirk M Zajonc[1]

Glycolipids presented by the major histocompatibility complex (MHC) class I homolog CD1d are recognized by natural killer T cells (NKT cells) characterized by either a semi-invariant T cell antigen receptor (TCR) repertoire (type I NKT cells or *i*NKT cells) or a relatively variable TCR repertoire (type II NKT cells). Here we describe the structure of a type II NKT cell TCR in complex with CD1d-lysosulfatide. Both TCR α-chains and TCR β-chains made contact with the CD1d molecule with a diagonal footprint, typical of MHC-TCR interactions, whereas the antigen was recognized exclusively with a single TCR chain, similar to the *i*NKT cell TCR. Type II NKT cell TCRs, therefore, recognize CD1d-sulfatide complexes by a distinct recognition mechanism characterized by the TCR-binding features of both *i*NKT cells and conventional peptide-reactive T cells.

Natural killer T cells (NKT cells) represent one of the most extensively studied unconventional lineages of T lymphocytes[1,2]. Characterization of this population has provided important insights related to the development and physiological role of innate-like T cells in immunity as well as the range of antigen-recognition mechanisms used by αβ T cell antigen receptors (TCRs). NKT cells reactive to antigens presented by CD1d can be categorized as type I or *i*NKT cells (which express a semi-invariant TCR characterized in mice by a conserved rearrangement of the α-chain variable region 14 and α-chain joining region 18 (V_α14-J_α18) paired with a limited repertoire of V_β chains, mainly V_β8.2, V_β7 and V_β2) and type II NKT cells (which express a more variable TCR repertoire). Lipid antigens bind to the CD1d groove, with their hydrophobic portion occupying the two main groove pockets (A′ and F′) and their polar portion exposed to the solvent[3]. Although the *i*NKT cell TCR can recognize both α-linked and β-linked glycolipids by forcing the antigens into a conserved conformation[4–7], type II NKT cells do not respond to α-linked glycolipids. Crystal structures of *i*NKT cell TCRs in complex with various CD1d-presented antigens have shown that the semi-invariant TCR docks with an unique mode, parallel to the CD1d antigen-binding groove, with most of the interface dominated by the germline-encoded α-chain[4,7,8]. The lack of a universal antigen for type II NKT cells, analogous to the potent *i*NKT cell TCR ligand α-galactosylceramide (α-GalCer)[9], has so far hampered understanding of the role of this cell population in normal states as well as in pathological states, despite the fact that type II NKT cells constitute a substantial portion of the $CD4^+$ T cells in mice deficient in major histocompatibility complex (MHC) class II (refs. 10,11) and in human bone marrow[12], liver[13] and gut[14]. Nonetheless, type II NKT cells reactive to the widely expressed self antigen sulfatide[15] have been found to be involved in the suppression of tumor immunity[16], regulation of ischemic reperfusion[17,18], experimental autoimmune encephalomyelitis[15], concanavalin A–induced hepatitis[19] and type 1 diabetes[20]. Notably, the finding that the administration of sulfatide protects mice from inflammatory disease in the central nervous system and liver in a manner dependent on type II NKT cells[15–20] suggests potential for the development of new agonists able to harness the immunomodulatory potential of this cell population. Sulfatide-reactive type II NKT cells use an oligoclonal repertoire with characteristics of both antigen-specific conventional T cells and innate-like T cells[21]. However, it is not known how these features of type II NKT cell TCRs determine the recognition of self antigen. We report here the crystal structure (at a resolution of 2.1 Å) of a type II NKT cell TCR (V_α1-J_α26 and V_β16-J_β2.1) isolated from the sulfatide-reactive, CD1d-restricted T cell hybridoma Hy19.3 (a subclone of the XV19 hybridoma)[15,22,23], as well as the crystal structure of the ternary complex of the TCR bound to mouse CD1d–lysosulfatide (LSF) at a resolution of 3.5 Å. LSF, which lacks the fatty-acid chain present on most sulfatide molecules, has been identified as the most potent antigen recognized by the Hy19.3 TCR[22,23], and high concentrations of LSF are found in tissues from people with metachromatic leukodystrophy[24]. The structural and biochemical data presented here describe how type II NKT cells recognize antigens by a distinct recognition mechanism, which provides a rationale for the TCR repertoire used by this population.

RESULTS

The Hy19.3 TCR binds diagonally above the CD1d A′ pocket

To investigate the structural basis of the recognition of sulfatide by type II NKT cells, we determined the crystal structure of the mouse

[1]Division of Cell Biology, La Jolla Institute for Allergy & Immunology, La Jolla, California, USA. [2]Laboratory of Autoimmunity, Torrey Pines Institute for Molecular Studies, San Diego, California, USA. Correspondence should be addressed to D.M.Z. (dzajonc@liai.org) or V.K. (vkumar@tpims.org).

Received 5 April; accepted 30 May; published online 22 July 2012; doi:10.1038/ni.2371

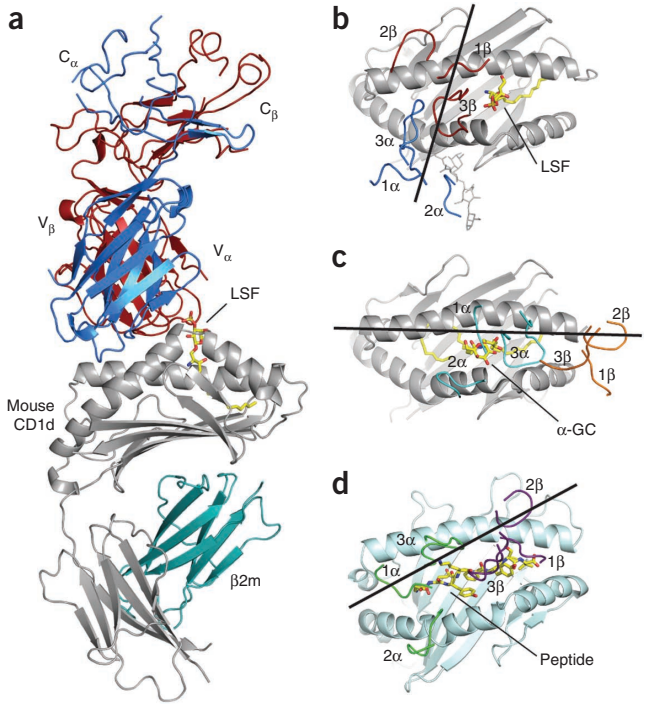

CD1d–LSF–Hy19.3 TCR complex at a resolution of 3.5 Å (**Fig. 1** and **Table 1**). Two highly similar ternary complexes (r.m.s. deviation of 0.7 Å over Cα atoms) were present in the asymmetric unit, and the following analysis was limited to one complex, unless otherwise stated. The electron density for both CD1d and the TCR at the complex interface was unambiguous (**Supplementary Fig. 1**). Strong density was present for the galactosyl moiety of LSF, whereas we observed relatively weak density for the sphingosine acyl chain modeled in the F′ pocket and a spacer occupying the A′ pocket (modeled as palmitic acid; **Supplementary Fig. 1**), similarly to what has been observed for the single alkyl-chain ligand lysophosphatidylcholine from the human CD1d–*i*NKT cell TCR complex[25]. The buried surface area of the CD1d-TCR was ~910 Å^2, slightly more than that of the *i*NKT cell TCR (~760 Å^2)[8] but below the range of values observed for MHC-TCR complexes (1,200–2,400 Å^2)[26]. The Hy19.3 TCR docked on the CD1d antigen-binding groove with an almost perpendicular orientation, roughly centered above the A′ pocket (**Fig. 1a**) with its V_α domain contacting the α2 helix (residues 154–167), whereas the V_β domain bound to the α1 helix (residues 68–79; **Fig. 1b**). This binding orientation was very different from that of the *i*NKT cell TCR, which bound above the opposite CD1d F′ pocket parallel to the CD1d α-helices[8] (**Fig. 1c**). We calculated the docking angle of the Hy19.3 TCR to be 74°, at the high end of the range of docking angles reported for MHC-TCR complexes (21–70°)[26]. Therefore, glycolipid-reactive type I and type II NKT cell TCRs mark the extreme ends of binding orientations of conventional peptide-MHC–reactive TCRs that typically bind diagonally above the antigen-presenting molecule, such as in the complex of the 2C TCR, H-2K^b MHC and dEV8 peptide[26,27] (**Fig. 1d**). Notably, the only known TCR with a higher docking angle (84°) is specific for a myelin protein–derived antigen[28]. This TCR also docked above the amino-terminal portion of the peptide corresponding to the A′ pocket (**Supplementary Fig. 2**), and it was proposed that this unusual binding mode allowed escape of negative selection[28]. Overall, the structure of the ternary complex showed that the Hy19.3 TCR docked on CD1d with an almost perpendicular orientation, which resulted in a footprint radically different from that of a previously described *i*NKT cell TCR.

Figure 1 Overall structure and docking orientation of the Hy19.3 TCR on the mouse CD1d–LSF complex. (**a**) Crystal structure of the mouse CD1d–LSF–Hy19.3 TCR complex: CD1d, gray; β_2-microglobulin (β_2m), aqua; TCR α-chain, blue; TCR β-chain, dark red; LSF, yellow. (**b**–**d**) TCR footprint and binding orientation of the mouse CD1d–LSF–Hy19.3 TCR complex (**b**), the mouse CD1d–α-GalCer–*i*NKT cell TCR complex (Protein Data Bank accession code 3HE6; **c**) and an MHC class I–peptide–TCR complex (Protein Data Bank accession code 2CKB; **d**). TCR α-chain, cyan (**c**) or green (**d**); TCR β-chain, orange (**c**) or purple (**d**). Black lines represent the vector that connect the centroids of the conserved disulfide bond in each V domain.

CDR1 and CDR2 contacts and the type II NKT cell repertoire

Both TCR chains made similar contributions to the interface with mouse CD1d in terms of buried surface area (α-chain, 49%; β chain, 51%). In contrast to the contacts made with the *i*NKT cell TCR, all six complementarity-determining region (CDR) loops contacted the mouse CD1d-LSF complex (**Fig. 2**). Specific residues on the germline-encoded CDR1 and CDR2 loops bound mouse CD1d, with CDR1β also contacting the antigen. In particular, residue Tyr33α of CDR1α, together with Phe52α, Ser53α and Asp54α of CDR2α, interacted with the α2 helix and an N-linked oligosaccharide (Asn165, **Fig. 2a**,**b**), whereas Tyr31β on CDR1β and Tyr50β of CDR2β contacted residues on the α1 helix (**Fig. 2e**,**f**). These loops contacted human and mouse CD1d in correspondence of two 'hot spots' identified before on the MHC protein surface (corresponding to Met69 of the α1 helix and Ala158 on the α2 helix), and two of the three residues equivalent to the 'restriction triad' always contacted by MHC-reactive TCRs[2] were also contacted by the Hy19.3 TCR (His68 and Val72; **Supplementary Table 1**), which resulted in the diagonal, albeit shifted, docking mode typical of MHC-TCR interactions[29]. Notably, among the mouse V_β segments, only V_β16, V_β8.1 and V_β8.3 have the combination of critical residues used to contact mouse CD1d–LSF (His30, Tyr31 and Tyr50), whereas only V_α1, V_α3, V_α5 and V_α8 have the combination of Tyr33 or Phe33 and Tyr52 in contact with the α2 helix. Notably, these represent most V segments identified in type II NKT cells[11] and

Table 1 Data collection and refinement statistics (molecular replacement)

	mCD1d-LSF-Hy19.3	Hy19.3
Data collection		
Space group	$P2_1$	$P2_12_12_1$
Cell dimensions		
a, *b*, *c* (Å)	98.51, 126.99, 104.35	73.22, 101.53, 134.49
α, β, γ (°)	90.00, 110.5, 90.00	90.00, 90.00, 90.00
Resolution (Å)	92.3–3.5 (3.69–3.50)	49.0–2.1 (2.15–2.1)
R_{merge} (%)	24.0 (81.4)	7.9 (56.3)
R_{meas} (%)	25.5 (86.5)	9.0 (64.3)
$R_{p.i.m.}$ (%)	8.7 (29.2)	4.2 (30.3)
Average I / σI	8.3 (2.8)	11.5 (2.5)
Completeness (%)	99.9 (99.9)	99.9 (99.9)
Redundancy	8.3 (8.5)	4.3 (4.2)
Refinement		
Resolution (Å)	92.3–3.5	38.0–2.1
Reflections	29,051	56,586
R_{work} / R_{free}	0.210 / 0.266	0.188 / 0.227
Ramachandran plot (%)		
Favored	91.3	97.6
Allowed	98.9	99.9
R.m.s. deviations		
Bond length (Å)	0.007	0.007
Bond angle (°)	1.11	1.04

One crystal was used for each structure. Values in parentheses are for the shell of highest resolution. R_{merge}, merging R factor; R_{meas}, measurement R factor; $R_{p.i.m.}$, precision-indicating merging R factor.

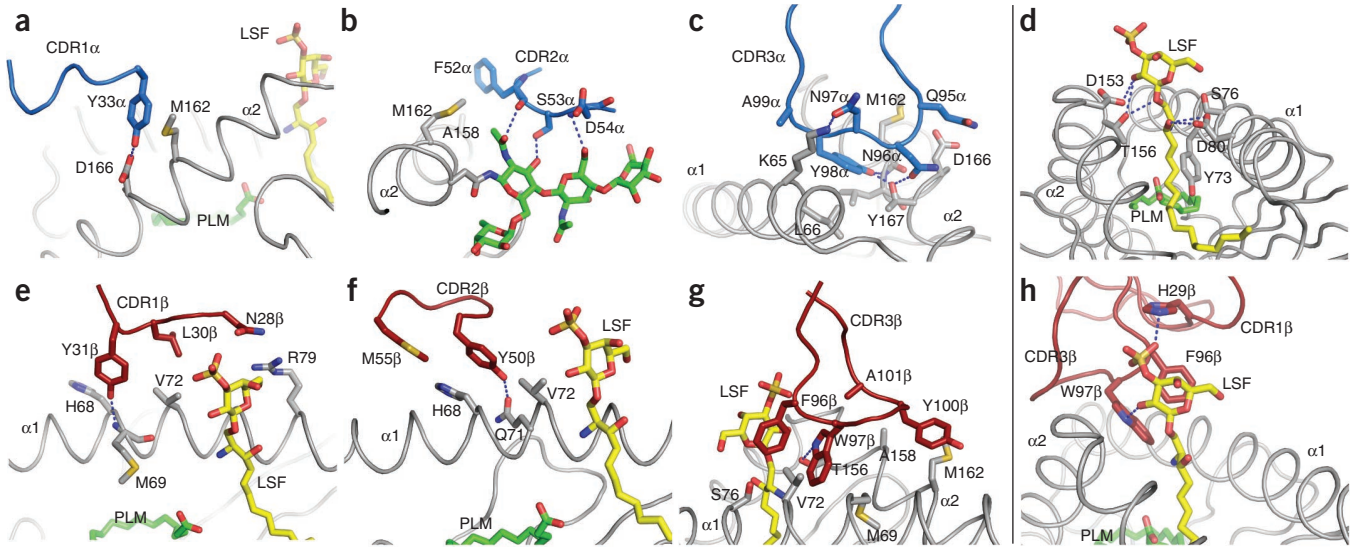

Figure 2 The CD1d-antigen-TCR interface. (**a**–**c**) Contacts between the TCR α-chain CDR loops (blue) and CD1d (gray): CDR1α (**a**), CDR2α (**b**) or CDR3α (**c**). (**b**) The N-linked glycosylation (green) at Asn165 of CD1d in contact with the CDR2α loop; dashed blue lines indicate polar contacts. (**d**) Contacts between CD1d (gray) and LSF (yellow). (**e**–**g**) Contacts between CD1d (gray) and the TCR β-chain CDR loops (dark red): CDR1β (**e**), CDR2β (**f**) or CDR3β (**g**). (**h**) Recognition of LSF (yellow) by the CDR1β and CDR3β loops of the Hy19.3 TCR (dark red). Green indicates the spacer lipid in the A′ pocket (palmitic acid (PLM)). Dashed blue lines indicate polar contacts.

in particular among sulfatide-reactive ones[21], which suggests a conserved docking mode for type II NKT cell TCRs. Thus, the requirement for specific contacts between the CDR1 and CDR2 loops and the mouse CD1d α1 and α2 helices observed for the Hy19.3 TCR provides an explanation for the TCR repertoire used by type II NKT cells.

Both CDR3α and CDR3β are critical for complex formation

The Hy19.3 TCR bound to mouse CD1d–LSF with micromolar affinity, as measured by surface plasmon resonance (**Fig. 3a**). The binding was characterized by relatively slow on rates and fast off rates, not dissimilar to what has been reported for interactions between weak *i*NKT cell antigens and MHC-TCR[30]. As most of the interface contacts in the ternary complex were mediated by the CDR3 loops not encoded by the germline (CDR3α and CDR3β accounted for 34% and 32% of the total buried surface area, respectively), we next determined whether substitution of residues on those two loops affected binding of the TCR. Consistent with the proposal of a pivotal role for the CDR3 loops at the CD1d-TCR interface, substitution of any of

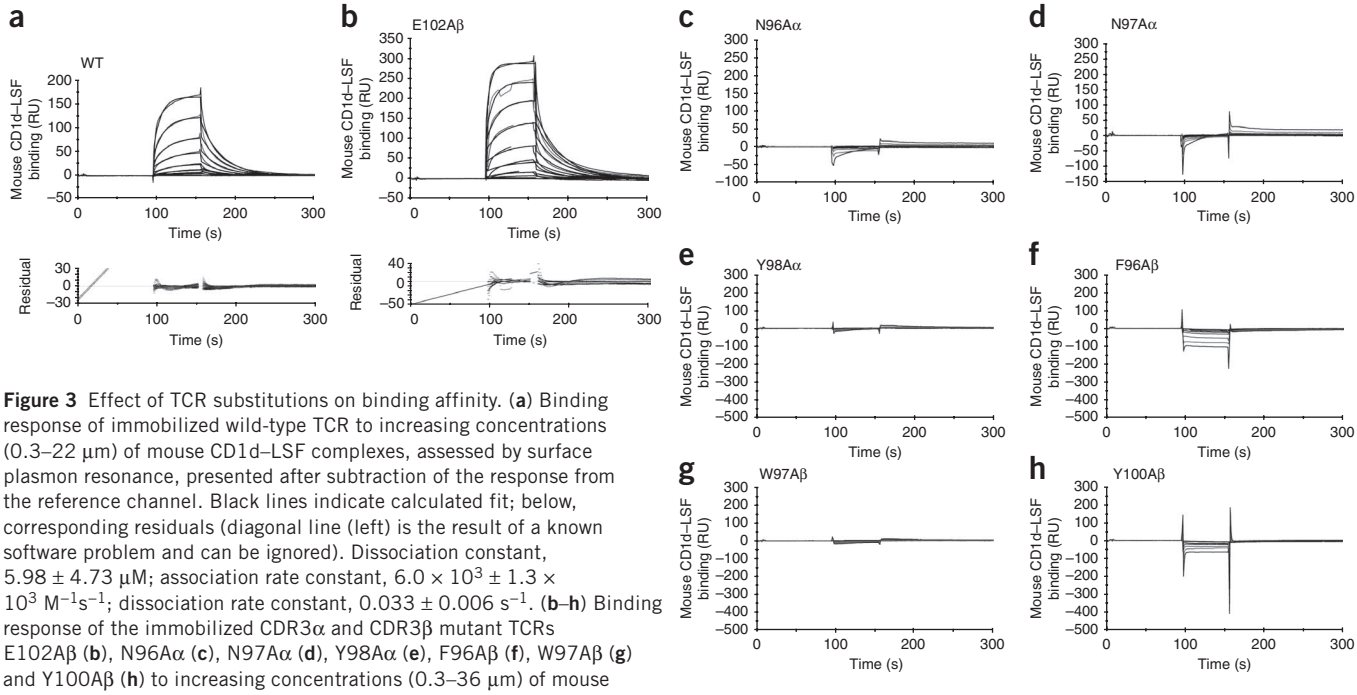

Figure 3 Effect of TCR substitutions on binding affinity. (**a**) Binding response of immobilized wild-type TCR to increasing concentrations (0.3–22 μm) of mouse CD1d–LSF complexes, assessed by surface plasmon resonance, presented after subtraction of the response from the reference channel. Black lines indicate calculated fit; below, corresponding residuals (diagonal line (left) is the result of a known software problem and can be ignored). Dissociation constant, 5.98 ± 4.73 μM; association rate constant, $6.0 \times 10^3 \pm 1.3 \times 10^3$ $M^{-1}s^{-1}$; dissociation rate constant, 0.033 ± 0.006 s^{-1}. (**b**–**h**) Binding response of the immobilized CDR3α and CDR3β mutant TCRs E102Aβ (**b**), N96Aα (**c**), N97Aα (**d**), Y98Aα (**e**), F96Aβ (**f**), W97Aβ (**g**) and Y100Aβ (**h**) to increasing concentrations (0.3–36 μm) of mouse CD1d–LSF complexes, assessed by surface plasmon resonance. E102Aβ values: dissociation constant, 6.65 ± 3.18 μM; association rate constant, $4.9 \times 10^3 \pm 2.0 \times 10^3$ $M^{-1}s^{-1}$; dissociation rate constant, 0.029 ± 0.003 s^{-1}. Data are from at least two independent experiments (average and s.d.).

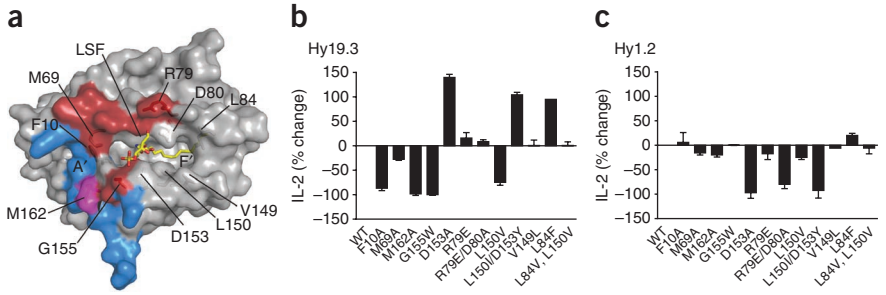

Figure 4 Substitution of CD1d residues at the interface affects activation of the Hy19.3 hybridoma. (**a**) Localization of mutant CD1d residues at the mouse CD1d–TCR interface: CD1d (gray surface) is presented with residues of the α-chain (blue) or β-chain (dark red) footprint; magenta indicates the only residue shared by the two footprints (Met162); yellow, LSF. (**b**,**c**) Release of IL-2 (a measure of hybridoma activation) by Hy19.3 cells (**b**) or the *i*NKT cell hybridoma line Hy1.2 (**c**) after stimulation in a plate coated with wild-type mouse CD1d (WT) or various mouse CD1d mutants (horizontal axes) loaded with LSF (2 μg/ml; Hy19.3 (**b**)) or α-GalCer (0.5 μg/ml; Hy1.2 (**c**)) at an optimal concentration determined by antigen titration. Data are representative of at least five independent experiments (error bars, s.e.m.).

the residues at the tip of these two CDR loops with alanine (N96Aα, N97Aα, Y98Aα, F96Aβ, W97Aβ or Y100Aβ) resulted in abrogation of binding, as measured by surface plasmon resonance, whereas the substitution in the control mutant E102Aβ did not have this effect (**Fig. 3b–h**). These results were reminiscent of what has been reported for MHC-reactive TCRs, for which both CDR3 loops have a critical role in complex formation, but was in contrast to results obtained with the *i*NKT cell TCR, for which CDR3β is thought to modulate only the affinity of the TCR for the CD1d-antigen complex[26,31].

Notably, the Hy19.3 TCR CDR3α loop exclusively contacted the mouse CD1d surface (**Fig. 2c**), whereas the CDR3β loop contacted both mouse CD1d and the antigen (**Fig. 2g**). A Gln95-Asn96-Asn97-Tyr98 motif on CDR3α bound to the top of the A′ roof of mouse CD1d, contacting both helices via polar and van der Waals contacts (**Supplementary Table 1**). The central Asn96-Asn97 motif observed on CDR3α is present on a sizeable proportion of sulfatide-reactive type II NKT cell TCRs[21] (**Supplementary Fig. 3**). Moreover, the length of the CDR3α of this TCR (ten amino acids) was similar to that of the highly restricted length of this loop in $V_α3$ and $V_α1$ sulfatide-reactive TCRs[21] and other type II NKT cells (eight to nine amino acids)[11]. Therefore, both CDR3α and CDR3β had a critical role in the formation of the ternary complex, with the interaction between mouse CD1d and CDR3α resulting in the oligoclonal nature of the CDR3α loops observed in type II NKT cells.

Substitution of the A′ pocket abolishes binding of Hy19.3 TCR

Substitution of selected amino-acid residues of mouse CD1d (**Fig. 4a**) showed that perturbation of the area around the A′ pocket (Phe10Ala, Met69Ala and Met162Ala) resulted in disruption of the mouse CD1d–Hy19.3 TCR interaction, as measured by an antigen-presentation assay (**Fig. 4b**). Those substitutions, however, did not substantially affect the binding of the *i*NKT cell TCR on the opposite side of mouse CD1d[4,7,8], above the F′ pocket (**Fig. 4c**). Notably, substitution of the aspartic acid at position 153 (which is crucial for the binding of *i*NKT antigens) with alanine or tyrosine resulted in more stimulation of the type II NKT hybridoma (**Fig. 4b**), which suggested that this residue was not involved in specific interactions with the antigen but instead impaired TCR recognition. As expected, residues around the F′ pocket were not crucial for the binding of Hy19.3 TCR, except for Leu150. However, as this residue was not near the Hy19.3 TCR, the substitution with alanine probably affected the binding of LSF to mouse CD1d. The presence of polymorphisms at CD1d residue 162 in laboratory and wild-type mouse strains have been shown to substantially affect the recognition of CD1d-antigen complexes by type II NKT cells[32]. In the ternary complex structure described here, the side chain of Met162 was capped by the aromatic residues Tyr33α, Phe52α and Tyr100β (**Supplementary Fig. 4**), which would provide an explanation for why modifications at this position can have direct consequences on the binding of the TCR. Notably, we also observed some degree of cross-species reactivity between human CD1d molecules and the Hy19.3 TCR, although to a lesser extent than with the *i*NKT cell TCR (**Supplementary Fig. 5**).

The Hy19.3 TCR recognizes LSF exclusively via the β-chain

The side chain of His29β on CDR1β contacted the sulfate group of LSF, whereas the bulky side chains Phe96β and Trp97β on CDR3β pinned the galactosyl residue against Asp153 on the mouse CD1d α2 helix (**Fig. 2h**), which would explain the 'preference' of this TCR for the extended-ligand conformation typical of β-linked glycolipids. This rather nonspecific binding mode suggested that modifications at the 4′ and 6′ positions of the hexose moiety would probably be tolerated. Moreover, comparison of the binding orientation of LSF and the closely related *cis*-tetracosenoyl sulfatide that we had crystallized bound to mouse CD1d in the absence of any TCR[33] (**Supplementary Fig. 6**) showed that they had considerable similarity, which further suggested that this TCR was able to bind several CD1d-ligand complexes with a conserved mode of recognition[23]. Notably, LSF was shifted by approximately 3 Å toward the F′ pocket, probably as a result of the presence of the bulky Trp97 of CDR3β (**Supplementary Fig. 6**). Furthermore, whereas the 'lyso' isoforms of sulfatide and glucosylceramide were the main antigenic lipids able to stimulate Hy19.3 cells when presented by splenocytes (**Fig. 5a**), several dual–alkyl chain β-linked glycolipids, such as various forms of sulfatide (with $C_{16:0}$, $C_{24:0}$ and $C_{24:1}$ acyl chains) and β-GalCer, were also recognized

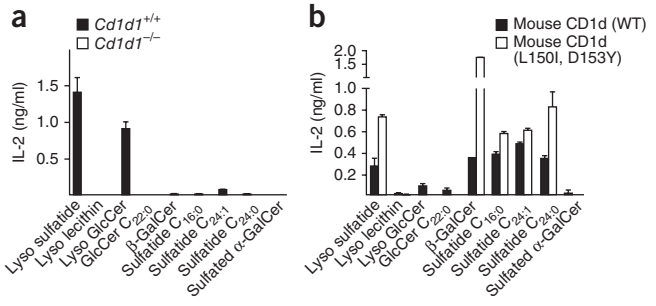

Figure 5 Recognition of self lipids by the Hy19.3 TCR. (**a**) Stimulation of NKT cells by various antigens (horizontal axis; 2.5 μg/ml each) in the presence of antigen-presenting cells (splenocytes) from wild-type mice (*Cd1d1*$^{+/+}$) or CD1d-deficient mice (*Cd1d1*$^{-/-}$), assessed as IL-2 release. GlcCer, glucosylceramide. (**b**) Stimulation of NKT cells by various antigens (horizontal axis) in plates coated with recombinant wild-type mouse CD1d or mutant mouse CD1d (L150I, D153Y) in the absence of antigen-presenting cells (presented as in **a**). Data are representative of three independent experiments (error bars, s.e.m.).

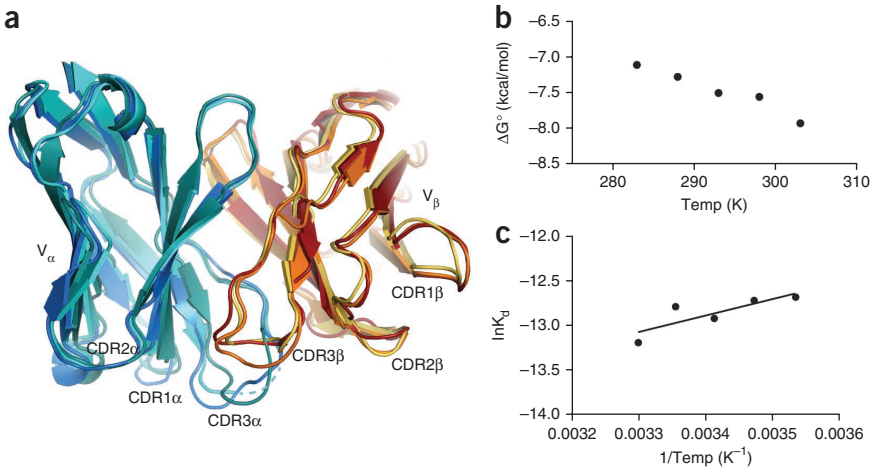

Figure 6 Flexibility in the CDR loops of the Hy19.3 TCR. (**a**) Superposition of TCR structures in complex and not in complex, showing V_α (in complex, blue; not in complex, cyan and aqua) and V_β (in complex, dark red; not in complex, orange and yellow); dashed line indicates the disordered portion of the CDR3α loop in one of the TCRs not in complex. (**b**) Free energy (ΔG) values of the mouse CD1d–LSF–Hy19.3 TCR complex at a range of temperatures. (**c**) Binding of the Hy19.3 TCR to mouse CD1d–LSF, with the enthalpic and entropic energetic contributions to the complex formation estimated by linear-regression of data from a van't Hoff plot yielding an enthalpy change (ΔH) value of 3.63 ± 3.58 kcal/mol and a temperature × change in entropy (TΔS) value of 11.28 ± 3.65 kcal/mol at 25 °C. Data are from two independent experiments (average).

when presented by plate-bound recombinant mouse CD1d (**Fig. 5b**). Substitution of Asp153 or Leu150 generally enhanced the antigenicity of most lipids (**Fig. 5b**). The lack of antigenicity observed for lysolecithin (lysophospatidylcholine) was probably the result of the considerable difference between the polar moiety (a phosphorylcholine group) of this lipid and that of the other antigens that carry hexose sugars. Moreover, the differences between plate-bound mouse CD1d and antigen-presenting cells in antigen presentation suggested that antigen-presenting cells either process antigens into an inactive form or prevent their presentation at the cell surface, consistent with the reported requirement for the trafficking of mouse CD1d to the lysosomal compartment for activation of type II NKT cells[22,34].

Flexibility in the Hy19.3 TCR and binding thermodynamics

We also determined the structure of the Hy19.3 TCR alone at a resolution of 2.1 Å (**Table 1**) and compared it with the structure of the same TCR in the ternary complex. Superposition of the two TCR structures not in complex present in the asymmetric unit onto the TCR conformation observed in the ternary complex showed flexibility in the CDR1α, CDR2β and CDR3 loops (**Fig. 6a**), which would potentially allow the TCR to recognize an even broader spectrum of antigens through fine positioning of the CDR footprint, as has been reported for some MHC-reactive TCRs[2]. That finding was in contrast to results obtained for the *i*NKT cell TCR, which binds to CD1d-presented antigens without substantial conformational changes in its CDR loops[4,8]. Also in contrast to the *i*NKT cell TCR[35], we observed that the binding affinity of the Hy19.3 TCR was temperature dependent (**Fig. 6b** and **Supplementary Fig. 7**). Notably, van't Hoff analysis of the binding data (**Fig. 6c**) suggested that the complex formation was driven entropically, possibly as a result of the hydrophobic interactions created at the CD1-TCR interface and/or water displacement (although the low resolution of the ternary complex did not allow us to model water molecules), similar to what has been reported, for example, for the complex of HLA-B8, FLR peptide and the 13 TCR[36].

DISCUSSION

The mouse CD1d–LSF–Hy19.3 TCR structure reported here has provided insight into the recognition of a lipid antigen by a non-invariant NKT cell TCR. Unexpectedly, the binding mode for the Hy19.3 TCR combined features of both *i*NKT cells and MHC-restricted T cells, which resulted in a unique antigen-recognition mechanism among αβ TCRs. In the type II NKT ternary complex, both the TCR α-chain and TCR β-chain contact the CD1d molecule with a diagonal footprint, typical of MHC-TCR interactions[26]. For peptide-MHC–reactive T cells, optimal T cell activation occurs when the coreceptor is engaged, which correlates with a limited range of TCR docking angles[37]. However, as NKT cells can be double-negative for expression of the CD4 and CD8 coreceptors[1], the angle at which the TCR docks on CD1d is not influenced by the engagement of coreceptors; thus, its importance in T cell activation remains unclear. However, the Hy19.3 TCR recognized the antigen exclusively with only one TCR chain, similar to the *i*NKT cell TCR[4,8], whereas MHC-reactive TCRs need both CDR3 loops to contact the antigen[26]. Unlike the *i*NKT cell TCR, which contacts the ligand with its α-chain, the type II NKT cell TCR bound lysosulfatide solely through the TCR β-chain, which suggested that the latter chain was responsible for the fine antigen specificity of the TCR. Consistent with that, oligoclonal use of V_β and variability in the length and sequence of the CDR3β loop have been observed in sulfatide-reactive NKT cells[21]. The role of the CDR1β and His29 in particular seemed less critical, as antigens that lack a sulfate group, such as β-GalCer and 'lyso' isoforms of glucosylceramide, were still recognized by this TCR. The conservation of key CDR1- and CDR2-interacting residues in lysosulfatide-reactive TCR and other sulfatide-reactive TCRs[21] suggests a shared recognition 'logic' for this class of self antigens that could extend to a substantial proportion of type II NKT cells[11]. Moreover, the finding that the CDR3α loop was not directly involved in antigen recognition but instead recognized the CD1d surface provides an explanation for the restricted length and conserved motifs observed on the CDR3α loop of most sulfatide-reactive and type II NKT cell TCRs. We hypothesize that rearrangement of the TCR α-chain is not a result of positive selection by a self antigen, as is true for *i*NKT cells, but is instead driven by binding to the nonpolymorphic CD1d molecule, consistent with the presence of sulfatide-reactive type II NKT cells in mice deficient in sulfatide[15,21–23]. Collectively, our data suggest that the immune system developed two very different strategies that enable the 'nonpolymorphic' CD1d to bind at least two different types of NKT cell TCRs. The finding that a substantial proportion of type II NKT cells respond to the myelin-derived glycolipid sulfatide[15] has been pivotal in determining the role of these cells in normal processes as well as in pathological processes. Given the growing recognition of the role of sulfatide-reactive type II NKT cells in the suppression of tumor immunity and regulation of autoimmune diseases[15–20], with the consequent therapeutic potential, the structure described here opens the way to the rational development of new ligands with immunomodulatory potential.

METHODS

Methods and any associated references are available in the online version of the paper.

Accession codes. GenBank: Hy19.3 TCR V_α sequence, JQ926734, and Hy19.3 TCR V_β sequence, JQ926735; Protein Data Bank: atomic coordinates and structure factors, 4ELK and 4ELM.

Note: Supplementary information is available in the online version of the paper.

ACKNOWLEDGMENTS

We thank the Stanford Synchrotron Radiation Lightsource (beamline 7-1) and the Advanced Light Source (beamline 5.0.3) for support during remote collection of data; M. Kronenberg (La Jolla Institute for Allergy & Immunology) for several CD1d mutants; R. Stanfield (The Scripps Research Institute) for computer scripts used for the measurement of docking angles; and N. Vu and J. Nourblin (La Jolla Institute for Allergy & Immunology) for help during cloning and protein expression. Supported by the US National Institutes of Health (AI074952 to D.M.Z. and CA100660 to V.K.), the Juvenile Diabetes Research Foundation (V.K.) and the Multiple Sclerosis National Research Institute (V.K.).

AUTHOR CONTRIBUTIONS

E.G. generated the TCR constructs, purified and crystallized the proteins, determined the structures and did surface plasmon resonance experiments; I.M. did the antigen-presentation assays; J.W. and P.I. provided assistance with mutant generation and protein purification; T.-T.M. sequenced the TCR; and E.G., V.K. and D.M.Z. analyzed the data and wrote the manuscript.

COMPETING FINANCIAL INTERESTS

The authors declare no competing financial interests.

Published online at http://www.nature.com/doifinder/10.1038/ni.2371.
Reprints and permissions information is available online at http://www.nature.com/reprints/index.html.

1. Godfrey, D.I., Macdonald, H.R., Kronenberg, M., Smyth, M.J. & Van Kaer, L. NKT cells: what's in a name? *Nat. Rev. Immunol.* **4**, 231–237 (2004).
2. Godfrey, D.I., Rossjohn, J. & Mccluskey, J. The fidelity, occasional promiscuity, and versatility of T cell receptor recognition. *Immunity* **28**, 304–314 (2008).
3. Zajonc, D. & Wilson, I.A. Architecture of CD1 proteins. *Curr. Top. Microbiol. Immunol.* **314**, 27–50 (2007).
4. Borg, N.A. *et al.* CD1d-lipid-antigen recognition by the semi-invariant NKT T-cell receptor. *Nature* **448**, 44–49 (2007).
5. Pellicci, D.G. *et al.* Recognition of β-linked self glycolipids mediated by natural killer T cell antigen receptors. *Nat. Immunol.* **12**, 827–833 (2011).
6. Yu, E.D., Girardi, E., Wang, J. & Zajonc, D. Cutting edge: structural basis for the recognition of β-linked glycolipid antigens by invariant NKT cells. *J. Immunol.* **187**, 2079–2083 (2011).
7. Li, Y. *et al.* The Vα14 invariant natural killer T cell TCR forces microbial glycolipids and CD1d into a conserved binding mode. *J. Exp. Med.* **207**, 2383–2393 (2010).
8. Pellicci, D.G. *et al.* Differential recognition of CD1d-α-galactosyl ceramide by the Vβ8.2 and Vβ7 semi-invariant NKT T cell receptors. *Immunity* **31**, 47–59 (2009).
9. Kawano, T. *et al.* CD1d-restricted and TCR-mediated activation of vα14 NKT cells by glycosylceramides. *Science* **278**, 1626–1629 (1997).
10. Cardell, S. *et al.* CD1-restricted $CD4^+$ T cells in major histocompatibility complex class II-deficient mice. *J. Exp. Med.* **182**, 993–1004 (1995).
11. Park, S.H. *et al.* The mouse CD1d-restricted repertoire is dominated by a few autoreactive T cell receptor families. *J. Exp. Med.* **193**, 893–904 (2001).
12. Exley, M.A. *et al.* A major fraction of human bone marrow lymphocytes are Th2-like CD1d-reactive T cells that can suppress mixed lymphocyte responses. *J. Immunol.* **167**, 5531–5534 (2001).
13. Exley, M.A. *et al.* Cutting edge: compartmentalization of Th1-like noninvariant CD1d-reactive T cells in hepatitis C virus-infected liver. *J. Immunol.* **168**, 1519–1523 (2002).
14. Fuss, I.J. *et al.* Nonclassical CD1d-restricted NK T cells that produce IL-13 characterize an atypical Th2 response in ulcerative colitis. *J. Clin. Invest.* **113**, 1490–1497 (2004).
15. Jahng, A. *et al.* Prevention of autoimmunity by targeting a distinct, noninvariant CD1d-reactive T cell population reactive to sulfatide. *J. Exp. Med.* **199**, 947–957 (2004).
16. Terabe, M. & Berzofsky, J.A. NKT cells in immunoregulation of tumor immunity: a new immunoregulatory axis. *Trends Immunol.* **28**, 491–496 (2007).
17. Arrenberg, P., Maricic, I. & Kumar, V. Sulfatide-mediated activation of type II natural killer T cells prevents hepatic ischemic reperfusion injury in mice. *Gastroenterology* **140**, 646–655 (2011).
18. Yang, S.H. *et al.* Sulfatide-reactive natural killer T cells abrogate ischemia-reperfusion injury. *J. Am. Soc. Nephrol.* **22**, 1305–1314 (2011).
19. Halder, R.C., Aguilera, C., Maricic, I. & Kumar, V. Type II NKT cell-mediated anergy induction in type I NKT cells prevents inflammatory liver disease. *J. Clin. Invest.* **117**, 2302–2312 (2007).
20. Subramanian, L. *et al.* NKT cells stimulated by long fatty acyl chain sulfatides protect against type 1 diabetes in nonobese diabetic mice. *PLoS ONE* **7**, e377771 (2012).
21. Arrenberg, P., Halder, R., Dai, Y., Maricic, I. & Kumar, V. Oligoclonality and innate-like features in the TCR repertoire of type II NKT cells reactive to a β-linked self-glycolipid. *Proc. Natl. Acad. Sci. USA* **107**, 10984–10989 (2010).
22. Roy, K.C. *et al.* Involvement of secretory and endosomal compartments in presentation of an exogenous self-glycolipid to type II NKT cells. *J. Immunol.* **180**, 2942–2950 (2008).
23. Blomqvist, M. *et al.* Multiple tissue-specific isoforms of sulfatide activate CD1d-restricted type II NKT cells. *Eur. J. Immunol.* **39**, 1726–1735 (2009).
24. Toda, K. *et al.* Lysosulfatide (sulfogalactosylsphingosine) accumulation in tissues from patients with metachromatic leukodystrophy. *J. Neurochem.* **55**, 1585–1591 (1990).
25. López-Sagaseta, J., Sibener, L.V., Kung, J.E., Gumperz, J. & Adams, E.J. Lysophospholipid presentation by CD1d and recognition by a human natural killer T-cell receptor. *EMBO J.* **31**, 2047–2059 (2012).
26. Rudolph, M.G., Stanfield, R.L. & Wilson, I.A. How TCRs bind MHCs, peptides, and coreceptors. *Annu. Rev. Immunol.* **24**, 419–466 (2006).
27. Garcia, K.C. *et al.* An alphabeta T cell receptor structure at 2.5 A and its orientation in the TCR-MHC complex. *Science* **274**, 209–219 (1996).
28. Hahn, M., Nicholson, M.J., Pyrdol, J. & Wucherpfennig, K.W. Unconventional topology of self peptide-major histocompatibility complex binding by a human autoimmune T cell receptor. *Nat. Immunol.* **6**, 490–496 (2005).
29. Marrack, P., Scott-Browne, J.P., Dai, S., Gapin, L. & Kappler, J.W. Evolutionarily conserved amino acids that control TCR-MHC interaction. *Annu. Rev. Immunol.* **26**, 171–203 (2008).
30. Joyce, S., Girardi, E. & Zajonc, D. NKT cell ligand recognition logic: molecular basis for a synaptic duet and transmission of inflammatory effectors. *J. Immunol.* **187**, 1081–1089 (2011).
31. Matulis, G. *et al.* Innate-like control of human iNKT cell autoreactivity via the hypervariable CDR3beta loop. *PLoS Biol.* **8**, e1000402 (2010).
32. Zimmer, M.I. *et al.* Polymorphisms in CD1d affect antigen presentation and the activation of CD1d-restricted T cells. *Proc. Natl. Acad. Sci. USA* **106**, 1909–1914 (2009).
33. Zajonc, D. *et al.* Structural basis for CD1d presentation of a sulfatide derived from myelin and its implications for autoimmunity. *J. Exp. Med.* **202**, 1517–1526 (2005).
34. Shin, J.H. *et al.* Mutation of a positively charged cytoplasmic motif within CD1d results in multiple defects in antigen presentation to NKT cells. *J. Immunol.* **188**, 2235–2243 (2012).
35. Cantu, C., Benlagha, K., Savage, P.B., Bendelac, A. & Teyton, L. The paradox of immune molecular recognition of α-galactosylceramide: low affinity, low specificity for CD1d, high affinity for αβ TCRs. *J. Immunol.* **170**, 4673–4682 (2003).
36. Ely, L.K. *et al.* Disparate thermodynamics governing T cell receptor-MHC-I interactions implicate extrinsic factors in guiding MHC restriction. *Proc. Natl. Acad. Sci. USA* **103**, 6641–6646 (2006).
37. Adams, J.J. *et al.* T cell receptor signaling is limited by docking geometry to peptide-major histocompatibility complex. *Immunity* **35**, 681–693 (2011).

ONLINE METHODS

Cloning, expression and purification of the Hy19.3 TCR and mouse CD1d. Total RNA was isolated from 5×10^6 hybridoma cells with an RNeasy Mini kit according to the manufacturer's instructions (Qiagen). First-strand cDNA synthesis of 5′ rapid amplification of cDNA ends and standard PCR (second-strand reaction) were done with a published protocol[38]. The PCR products were cloned into the pGEM-T easy vector (Promega) for sequencing and then subcloned in *Escherichia coli* expression vectors containing the human constant domains of either the α-chain or the β chain (pET22b+ for the gene segment encoding V_α1-J_α26; pET30a+ for the gene segment encoding V_β16-J_β2.1) as described for the *i*NKT cell TCR[39]. Fully glycosylated mouse CD1d protein was expressed and purified as described[39]. The α- and β-chains of the Hy19.3 TCR were expressed separately in *E. coli* BL21(DE3) cells as inclusion bodies, then were extracted with 6 M guanidine-HCl in 50 mM Tris-HCl, pH 7.0, 5 mM EDTA, 2 mM DTT. Then, 32 mg α-chain and 48 mg β-chain were mixed in presence of 1 mM DTT. The mixture was then added dropwise to 1 liter of refolding buffer with stirring at 4 °C (50 mM Tris-HCl, 0.4 M arginine, 5 M urea, 2 mM EDTA, 5 mM reduced glutathione, 0.5 mM oxidized glutathione and 0.2 mM PMSF, pH 8 at 25 °C). After 16 h, 32 mg α-chain and 32 mg β-chain were added to the refolding buffer and the mixture was stirred for an additional 8–10 h. The mixture was then dialyzed for ~16 h against 10 mM Tris-HCl, 0.1 M urea, pH 8.0, followed by dialysis for 24 h against 10 mM Tris-HCl, pH 8.0. DEAE sepharose beads (3 ml settled resin; GE Healthcare) were added to the refolding solution for 2–4 h before collection on an Econo column (Bio-Rad Laboratories). Refolded TCRs were eluted with 100–150 mM NaCl in 10 mM Tris, pH 8.0, and were further purified by anion-exchange chromatography (MonoQ 5/50 GL in 10 mM Tris, pH 8.0; GE Healthcare) with a linear gradient of NaCl (0–300 mM). Fractions containing the TCR were purified by gel-filtration chromatography (Superdex S200 10/300 GL, in 50 mM HEPES and 150 mM NaCl, pH 7.5; GE Healthcare) and were concentrated to 5 mg/ml for further analysis.

Lipid loading and complex formation. Lysosulfatide (Matreya) was dissolved in DMSO at a concentration of 4 mg/ml. Purified mouse CD1d was incubated for 16 h at 25 °C with lysosulfatide (at a molar excess of 3× to 6×) before further purification by gel-filtration chromatography (Superdex S200 10/300 GL in 50 mM HEPES, 150 mM NaCl, pH 7.5; GE Healthcare) for removal of excess lipid. The CD1d-LSF complex and the Hy19.3 TCR (at a molar ratio of 1:1 with each at a concentration of ~5 mg/ml) were then mixed and incubated for 1 h at 25 °C for the promotion of complex formation.

Crystallization and data collection. Crystals of the TCR were grown at 23 °C by sitting-drop vapor-diffusion mixture of 0.1 µl protein (5 mg/ml) with 0.1 µl precipitant (18% polyethylene glycol 3350 and 0.2 M ammonium citrate dibasic). Crystals of the ternary complex were grown over several weeks at 4 °C by sitting-drop vapor-diffusion during mixture of 1 µl protein (~5 mg/ml) with 1 µl precipitant (11% polyethylene glycol 4000, 4% tacsimate, pH 6). Crystals were flash-cooled at 100K in a solution containing the crystallization solution and 20% glycerol. Diffraction data were collected at the Stanford Synchrotron Radiation Lightsource beamline 7.1 (Hy19.3 TCR) or at the Advanced Light Source beamline 5.0.3 (ternary complex). The Hy19.3 TCR crystals belong to space group $P2_12_12_1$ with cell parameters a = 73.2 Å, b = 101.5 Å and c = 134.5 Å. The mouse CD1d–LSF–Hy19.3 TCR crystal belongs to space group $P2_1$ with cell parameters a = 98.5 Å, b = 127.0 Å and c = 104.4 Å β = 110.5°. Data were processed with the iMOSFLM graphical user interface to the diffraction data-integration program MOSLFM and the Scala scaling and data-merging program in the CCP4 suite (Collaborative Computational Project number 4)[40] (**Table 1**).

Structure determination and refinement. The two structures were solved by molecular replacement with the PHASER program for phasing macromolecular crystal structures by maximum-likelihood methods[41]. The structure of an *i*NKT cell TCR (PDB ID 2Q86) with its CDR loops removed was used as a template for the Hy19.3 TCR data, which yielded two molecules in the asymmetric unit. For the ternary complex, a search for mouse CD1d (Protein Data Bank accession code 3ILQ, with the ligand, water molecules and oligosaccharides removed) was completed first, which yielded two CD1d molecules. A search with Hy19.3 TCR structure not in complex, with its CDR loops removed, resulted in two TCR molecules in the asymmetric unit, for a total of two highly similar ternary complexes in the asymmetric unit (r.m.s. deviation of 0.7 Å on Cα atoms). For both structures, the REFMAC macromolecular refinement program[40] was used for refinement (with the software Phenix[42] used for the final cycles of refinement of the Hy19.3 TCR not in complex) with application of both translation, libration and screw rotation and noncrystallographic symmetry restraints, intercalated with cycles of manual building in the COOT program for macromolecular model building, completion and confirmation (Crystallographic Object-Oriented Toolkit)[43]. The final Hy19.3 TCR structure was refined to 2.1 Å with a final R / R_{free} value of 18.8 / 22.7% (Ramachandran allowed / favored residues, 97.6 / 99.9%), and the final ternary complex structure was refined to 3.5 Å with a final R / R_{free} value of 21.0 / 26.6% (Ramachandran allowed / favored residues, 91.3 / 98.9%). Refinement statistics are presented in **Table 1**.

Mutant generation. The CD1d mutants have been described[44,45]. Hy19.3 TCR mutants were generated by site-mutagenesis with the QuikChange II kit (Stratagene; Agilent Technologies) with primers designed on the QuikChange Primer Design server. Proteins were expressed and purified as the wild-type proteins were.

Antigen-presentation assays. CD1d mutants were assessed by a CD1d-coated-plate assay essentially as described[15,22]. For the antigen-presenting-cell assay, irradiated splenocytes from C57BL/6 and *Cd1d1*$^{-/-}$ mice were used. Synthetic and semisynthetic lipids (Matreya) have been described[15,21,22,33].

Surface plasmon resonance measurements. A Biacore3000 was used for measurement of the kinetics of surface plasmon resonance by immobilization of biotinylated Hy19.3 TCR (wild-type or mutant variants with a carboxy-terminal birA tag on the β-chain) on a sensor chip from a CAPture kit (GE Healthcare); increasing concentrations of purified mouse CD1d–LSF in 10 mM HEPES, pH 7.5, 150 mM NaCl and 3 mM EDTA were allowed to flow across the chip at a rate of 30 µl/min.

For studies of thermodynamics, 8 µM mouse CD1d–LSF was injected over immobilized wild-type TCRs at a range of temperatures from 10 °C to 30 °C in increments of 5 °C. Kinetic parameters were calculated by a simple Langmuir 1:1 model in BIAevaluation software version 4.1 (GE Healthcare). Enthalpic and entropic contributions to the binding were estimated by van't Hoff analysis. Data points were fitted by linear regression with GraphPad Prism software.

38. Yu, E.D. *et al.* Structural basis for the recognition of C20:2-αGalCer by the invariant natural killer T cell receptor-like antibody L363. *J. Biol. Chem.* **287**, 1269–1278 (2012).
39. Wang, J. *et al.* Lipid binding orientation within CD1d affects recognition of Borrelia burgorferi antigens by NKT cells. *Proc. Natl. Acad. Sci. USA* **107**, 1535–1540 (2010).
40. Winn, M.D. *et al.* Overview of the CCP4 suite and current developments. *Acta Crystallogr. D Biol. Crystallogr.* **67**, 235–242 (2011).
41. McCoy, A.J. *et al.* Phaser crystallographic software. *J. Appl. Crystallogr.* **40**, 658–674 (2007).
42. Adams, P.D. *et al.* PHENIX: a comprehensive Python-based system for macromolecular structure solution. *Acta Crystallogr. D Biol. Crystallogr.* **66**, 213–221 (2010).
43. Emsley, P., Lohkamp, B., Scott, W.G. & Cowtan, K. Features and development of Coot. *Acta Crystallogr. D Biol. Crystallogr.* **66**, 486–501 (2010).
44. Burdin, N. *et al.* Structural requirements for antigen presentation by mouse CD1. *Proc. Natl. Acad. Sci. USA* **97**, 10156–10161 (2000).
45. Girardi, E. *et al.* Unique interplay between sugar and lipid in determining the antigenic potency of bacterial antigens for NKT cells. *PLoS Biol.* **9**, e1001189 (2011).